Journal of Hydroscience and Hydraulic Engineering
Vol. 3, No. 1, April, 1985, pp.63-74.

TRANSITION IN THE BEHAVIOR OF SEDIMENT LADEN VERTICAL BUOYANT JET

By

Yoich Awaya
Department of Civil Engineering Hydraulics and Soil Mechanics,
Kyushu University, Fukuoka 812, Japan

Kazuhiro Fujisaki and Kiyofumi Matsunaga

Department of Civil Engineering,
Kyushu Institute of Technology, Tobata-ku, Kitakyushu 804, Japan

SYNOPSIS

The sediment laden buoyant jets with a certain fall velocity of particles are analyzed theoretically, assuming similarities for both velocity and sediment concentration profiles, and using Prandtl's mixing-length theory, for two-dimensional and axisymmetric cases.

The jets are shown to be divided into three regions: nonbuoyant region, plume region, and settling region which causes only in an axisymmetric case.

The numerical solutions show that the particle laden jet performs like a pure jet near the jet source, as the initial momentum is predominant. For the two-dimensional jet, the jet becomes asymptotic to the negative buoyant plume of finite velocity which is expressed in terms of jet sediment flux. For the round jet, the velocity of plume decreases continuously, so the plume turns to the next stage where particles settling is predominant.

The validity of numerical solutions are checked by laboratry experiments.

INTRODUCTION

This paper concerns sediment laden jet which is injected vertically into calm water of uniform density. The jet spreads like a pure jet near the jet source, as the initial momentum of a jet is predominant. Then the jet turns to the density plume as the flow velocity decays and for the axisymmetric case the velocity of plume decreases continuously.

In this paper, we discuss the effect of initial momentum and particle flux of jet on the buoyant jet behavior. The main objective of this study is to investigate the effect of particle fall velocity and the effect of sediment concentration on the buoyant jet characteristics.

In the theoretical investigations, the mixing length model is adapted to the turbulent diffusion. The similarity profiles of jet flow velocity and sediment concentration in a cross section are also assumed.

Several works have been reported on the sediment laden vertical jet. Kikkawa et al. (5), Brush(2), and Singamsetti(13) discussed on the case where jet momentum is predominant , while Kitano et al. (6) studied on the bubble plume where relative density of fluid is predominant and initial momentum is negligible. To the best of writers knowledge, however, there has been no study which treats the particle laden jet characteristics including the transition behavior mentioned above.

There are some other papers concerning the buoyant jet or plume, such as by Morton (10), Abraham (1), Kotsovinos (7) which treat the buoyant jet of different density from ambient fluid. Making use of the results of those previous works, we discussed the value of numerical parameter which relates the mixing length to the jet breadth.

Numerical solutions given by the basic equations are checked by experiments.

THEORETICAL INVESTIGATION

Basic equations

The excess specific gravity due to particle suspension is given by

$$\sigma = c(\rho_s - \rho_1)/\rho_1$$

where ρ_s is the density of suspended particles, ρ_1 is the density of fluid, C is the volume concentration of sediment particles.

In the derivation of the basic equation of the particle laden jet, the following assumptions are made about the particle motion. First, it is assumed that the relative motion of a particle adds no effect to the turbulence in a buoyant jet, and that the acceleration due to the turbulence which acts to a particle is negligibly small compared with the acceleration due to gravity, so that the relative motion of each particle to the surrounding fluid is only settling by its own fall velocity.

Fig, 1 shows schematic illustration of submerged jet. Taking x axis along the jet center and y axis across it, the equation of continuity, conservation of momentum and negative buoyancy flux of sediments are applied to yield the governing equations as follows

$$\frac{\partial u}{\partial x} + y^{-n}\frac{\partial (y^n v)}{\partial y} = 0 \qquad (1)$$

$$\frac{\partial u^2}{\partial x} + y^{-n}\frac{\partial (y^n uv)}{\partial y} = \sigma g + y^{-n}\frac{\partial}{\partial y}\{K_m y^n (\frac{\partial u}{\partial y})\} \qquad (2)$$

$$\frac{\partial}{\partial x}\{\sigma(u + w)\} + y^{-n}\frac{\partial}{\partial y}(y^n \sigma v) = y^{-n}\frac{\partial}{\partial y}\{K_s y^n (\frac{\partial \sigma}{\partial y})\} \qquad (3)$$

where u is the velocity in the x direction, v is the velocity in the y direction, w is the fall velocity of sediment particles, assumed to take a constant value which is not affected by the particle concentration.

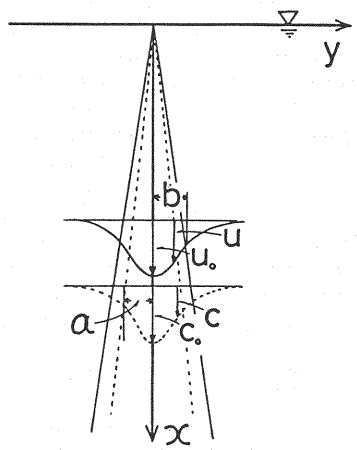

Fig.1 Schematic illustration of submerged jet

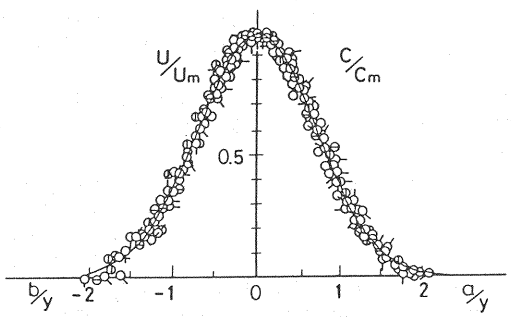

Fig.2 Profiles of velocity and sediment concentration symbols in the Figure are listed in table 3 (two-dimensional case)

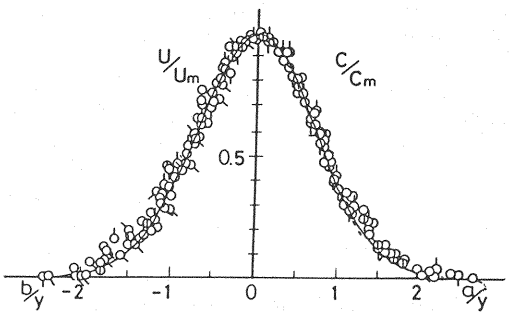

Fig.3 Profiles of velocity and sediment concentration symbols in the Figure are listed in table 4 (axisymmetric case)

Km is kinematic eddy viscosity and Ks is eddy diffusivity for sediment, and n=0 for a two-dimensional jet and n=1 for an axisymmetric one.

The buoyant jet is assumed to have Gaussian profiles of time mean vertical velocity and of time mean negative buoyancy, as shown in Fig.2 and Fig.3, then we obtain

$$u = u_0(x)\exp\{-y^2/b(x)^2\} \tag{4}$$

$$\sigma = \sigma_0(x)\exp\{-y^2/a(x)^2\} \tag{5}$$

where u_0 and σ_0 means a center line value of each variables, b(x) is the characteristic jet width of buoyant jet spreading, and a(x) is that of sediment spreading. The experimental values plotted in Figs.2 and 3 will be described later.

It is assumed that Ks is proportional to Km, so that $Ks = \beta Km$, and β is taken to be 1 because of the lack of sufficient knowledge on this subject so far, hereafter we write K=Km=Ks. We also assume that the momentum diffusion coefficient is described by the Boussinesq expression and the Prandtl's momentum transfer theory, thus

$$K = l^2\left|\frac{\partial u}{\partial y}\right| \quad , \qquad l = \varepsilon \cdot b \tag{6}$$

As our objective is to describe a gross jet behavior of the particle laden buoyant jet, the numerical value of the parameter ε is assumed to have a constant value along the jet.

As we assumed the Gaussian profiles of vertical velocity and vertical buoyancy previously, it is necessary to derive four ordinary differential equations relating to four variables $u_0(x)$, b(x), $\sigma_0(x)$ and a(x) from the three partial differential Eqs. 1,2 and 3. For this purpose, we integrated the basic Eqs.2 and 3.

In a case of two-dimensional buoyant jet, we can derive Eq.7 by integrating each term of Eq.2 over y from $-\infty$ to $+\infty$ with the use of Eq.1. Multiplying each term of Eq.2 by y and integrating over y from $-\infty$ to $+\infty$, we obtain Eq.9. The derivation of Eq.9 is shown in Appendix(I). Making use of the same way we also obtain Eq.8 and Eq.10 from Eq.3.

$$\frac{1}{\sqrt{2}}\frac{d}{dX}(U_0^2 B) = AS \tag{7}$$

$$\frac{d}{dX}\{SA(1 + \frac{U_0}{(1 + \lambda^2)^{1/2}})\} = 0 \tag{8}$$

$$(\pi + 4)U_0 B^2\frac{dU_0}{dX} + (\pi + 2)BU_0^2\frac{dB}{dX} = 2\sqrt{2\pi}BU_0^2 + 4A^2S \tag{9}$$

$$\{\tan^{-1}\lambda + \frac{\lambda}{1 + \lambda^2}\}SB\frac{dU_0}{dX} + \{\tan^{-1}\lambda + \frac{\lambda(\lambda^2 - 1)}{(1 + \lambda^2)^2}\}SU_0\frac{dB}{dX} + 2\{1 + \frac{U_0}{(1 + \lambda^2)^2}\}S\frac{dA}{dX}$$

$$+ \{1 + \frac{U_0}{(1 + \lambda^2)}\}A\frac{dS}{dX} = 2\sqrt{\pi}U_0 S\frac{1}{(1 + \lambda^2)^{3/2}} \tag{10}$$

where

$$\lambda = A/B \tag{11}$$

$$U_0 = u_0/w \ , \ X = x/L_0, \ B = b/(\varepsilon^2 L_0) \ , \ A = a/(\varepsilon^2 L_0) \ , \ S = \sigma_0 g L_0/w^2 \tag{12}$$

$$\left.\begin{aligned} L_0 &= m(qg)^{-2/3}(2/\pi)^{1/2}\varepsilon^{-2/3} \\ q &= 2\int_0^\infty \sigma(u + w)dy = \sqrt{\pi}a\sigma_0\{w + bu_0(a^2 + b^2)^{-1/2}\} \end{aligned}\right\} \tag{13}$$

$$M = m/(\sqrt{\pi/2}\varepsilon^2 L_0 w^2) = BU_0^2$$
$$Q = qg\varepsilon^{-2}w^{-3} = \sqrt{\pi}\, AS\{1 + BU_0/(A^2 + B^2)^{1/2}\} \qquad (14)$$

in which m is the jet momentum flux at the virtual origin

$$m = 2\int_0^\infty u^2 dy \qquad (\text{at } x=0)$$

In above nondimensional expressions, M is a momentum flux at the virtual point or line source. Q is the sediment particle flux. B and A correspond to the characteristic jet spread width of momentum and of sediment respectively, and Lo is a characteristic length which means the ratio of excess jet gravity to initial jet momentum.

In a case of axisymmetric buoyant jet, the following equations are derived from Eq.1 - Eq.6, with the same procedure as used in deriving Eqs.7, 8, 9 and 10. In this case the integration is made over the whole cross sectional area of the jet.

$$\frac{d}{dX}(U_0^2 B^2) = 2SA^2 \qquad (15)$$

$$\frac{d}{dX}\{SA^2(1 + \frac{U_0}{(1+\lambda^2)})\} = 0 \qquad (16)$$

$$B^3 U_0 \frac{dU_0}{dX} + \frac{2\sqrt{2} - 1}{\sqrt{2}} B^2 U_0^2 \frac{dB}{dX} = A^3 S + \frac{2}{\sqrt{\pi}} B^2 U_0^2 \qquad (17)$$

$$\{1 - \frac{1}{(1+\lambda^2)^{3/2}}\}AB^2 S \frac{dU_0}{dX} + \{2 - \frac{2}{(1+\lambda^2)^{3/2}} - \frac{3\lambda^2}{(1+\lambda^2)^{5/2}}\}ABSU_0 \frac{dB}{dX}$$
$$+ 3\{\frac{U_0}{(1+\lambda^2)^{5/2}} + 1\}A^2 S \frac{dA}{dX} + \{1 + \frac{U_0}{(1+\lambda^2)^{3/2}}\}A^3 \frac{dS}{dX} = \frac{8}{\sqrt{\pi}} \frac{\lambda^2}{(1+\lambda^2)^2} B^2 S U_0 \qquad (18)$$

where

$$U_0 = u_0/w \;,\; X = x/L_1 \;,\; B = b/(\varepsilon^2 L_1) \;,\; A = a/(\varepsilon^2 L_1)$$
$$S = \sigma_0 g L_1/w^2 \qquad (19)$$

$$L_1 = m^{3/4}(qg)^{-1/2}(2/\pi)^{3/4}\varepsilon^{-1}$$
$$q = \int_0^\infty 2\pi y(u + w)\sigma dy = \pi\sigma_0 a^2\{w + b^2 u_0/(a^2 + b^2)\} \qquad (20)$$

$$M = m/(\sqrt{\pi/2}\varepsilon^2 L_1 w)^2 = B^2 U_0^2$$
$$Q = qgL_1^{-1}w^{-3}\varepsilon^{-4} = \pi A^2 S(1 + U_0/(1+\lambda^2)) \qquad (21)$$

in which

$$m = \int_0^\infty 2\pi y u^2 dy \qquad (\text{at } x=0)$$

The jet behavior is assumed to be characterized by the initial jet momentum M and sediment flux Q, but the following relation is derived by substituting the first eqution of Eq.13 (or Eq.20) into Eq.14 (or Eq.21)

$$M = Q^{2/3}$$

This means that the jet behavior can be represented by only one parameter Q both in a two-dimensional case and in an axisymmetric case.

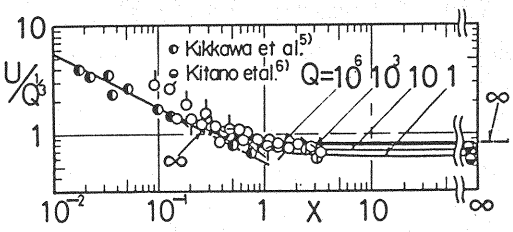

Fig.4 Decay of jet center-line velocity
(two-dimensional case)

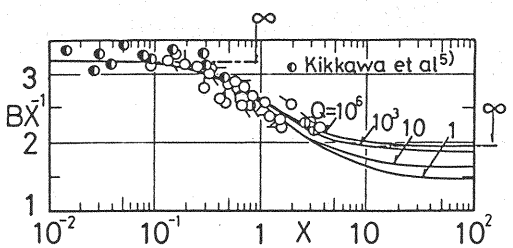

Fig.6-1 Jet spreading of momentum B
(two-dimensional case)

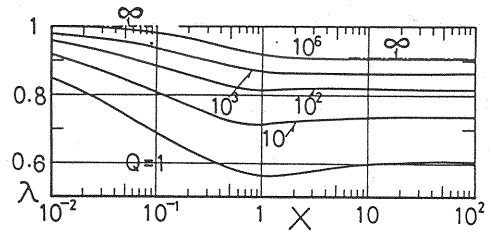

Fig. 7 Jet spreadig ratio $\lambda = A/B$
(two-dimensional case)

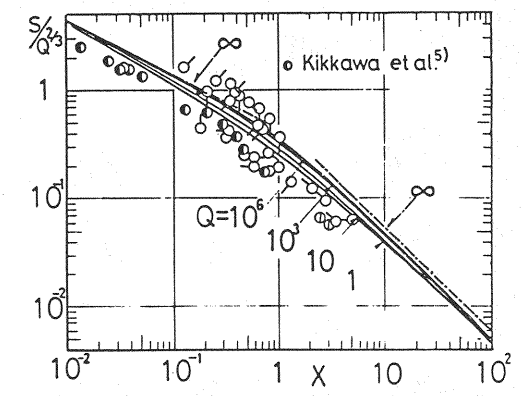

Fig.5 Decay of sediment concentration
(two-dimensional case)

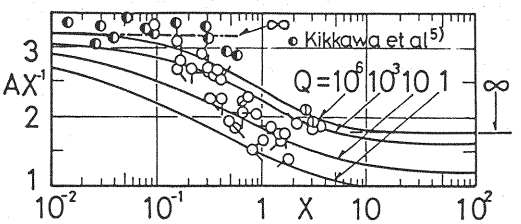

Fig.6-2 Jet spreading of sdiment A
(two-dimensional case)

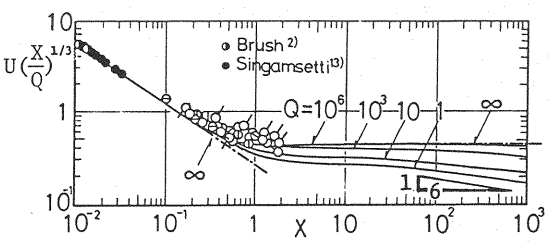

Fig.8 Decay of jet center-line velocity
(axisymmetric case)

Numerical Solutions

Numerical integrations of the basic equations are made by use of Runge-Kutta-Gill method. The values of four unknowns Uo, S, B, A are obtained along the jet succesively by solving Eqs.7-10 for the two-dimensional case.

Numerical solutions for two-dimensional case are shown in Fig.4 - Fig.7 together with experimental values.

Fig.4 and 5 show the decay of jet flow velocity and sediment concentrations along the jet center line, respectively. It is one of the most characteristic features of two-dimensional plume of this type that the center-line velocity of the plume becomes asymptotically to a constant value and this constant value is uniquly determined by the jet particle flux Q. On the other hand the sediment concentration decreases continuously along the jet axis X. In those Figures, $Q=\infty$ corresponds to the case of w=0.

The jet spreading with momentum B and factor A is shown in Fig.6 and Fig.7, where λ is the ratio of width of momentum jet to that of sediment.

In Fig.4-6,the transition behavior from jet like flow to plume like flow can be shown.

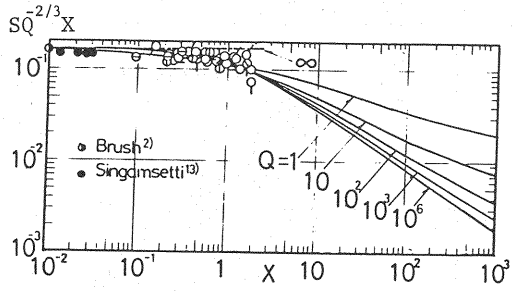

Fig.9 Decay of sediment cncentration (axisymmetric case)

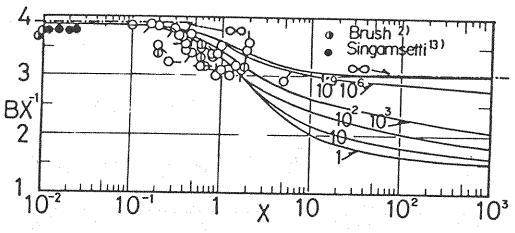

Fig.10-1 Jet spreading of momentum B (axisymmetric case)

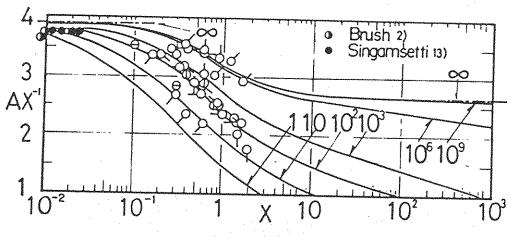

Fig.10-2 Jet spreading of sediment A (axisymmetric case)

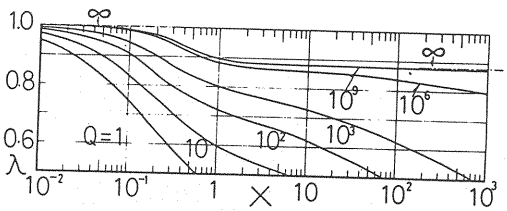

Fig.11 Jet spreading ratio $\lambda = A/B$ (axisymmetric case)

For the axisymmetric jet the numerical solution is obtained from Eqs.15 - 18 just like the same way as for the two-dimensional jet. These solutions are shown in Fig.8 - Fig.11.

Like a two-dimensional buoyant jet, the buoyant jet turns from the momentum predominant jet to the plume in which the relative density predominant. Furthermore, in an axisymmetric case, as the center-line velocity decreases continuously, the plume goes to the final stage where sediment particles settle down by their own fall velocity. Thus, in an axisymmetric case, the center-line velocity of the plume turns to zero. This is one of the remarkable difference compared with the two-dimensional case. The cause of this difference is just the same as in the case of pure plumes.

The jet center-line velocity decay in each stage is represented by $X^{-1}, X^{-1/3}, X^{-1/2}$ ($X^{-2/3}, X^{0}, X^{-1/6}$ in Fig.8) respectively. In Fig.8, for the case of Q=10 for example, in the region $X<1$: momentum is predominant, $5<X<50$: relative density is predominant and $X>10^2$: particle falling becomes effective. The same kind of transition behavior about some other properties of the buoyant jet is shown in Fig.9 and 10. When the values of Q are very small, the particle fall velocity becomes effective before the jet turns to the plume.

Discussion

In this study the mixing-length theory is employed, so the turbulent diffusivity is assumed to be determined by ε, jet width and jet center-line velocity. For the prediction of the jet behavior the values of ε must be determined. In order to determine the value of ε, which is taken to have a constant value over full jet range in this work, we assume the value of ε has almost the same value as that for w=0.

Numerical values of ε calculated from previous works are summarized in Table 1 and Table 2. The values of ε, which are shown in brackets in those tables, are calculated by equating the values of each jet properties in references to those of this work.

The following values of ε may be obtained from these tables; for two-dimensional case $\varepsilon=0.2$ for jet, $\varepsilon=0.3$ for plume, and for axisymmetric case $\varepsilon=0.18$ for jet, and $\varepsilon=0.2$ for plume. Morton (10) also assumed in their buoyant jet analysis that ε has constant value along jet, just like in our study. The numerical values in these tables will be helpful to describe the particle-laden jet behavior.

Table 1 Comparison of liquid buoyant jet (two-dimensional case)

	Jet				Plume			
	$\frac{b}{x}$	$\frac{a}{x}$	$\frac{u_0\sqrt{x}}{\sqrt{m}}$	$\frac{\sigma_0\sqrt{x}}{g\sqrt{m}}$	$\frac{b}{x}$	$\frac{a}{x}$	$\frac{u_0}{(qg)^{1/3}}$	$\frac{\sigma_0 gx}{(qg)^{2/3}}$
Authors	$3.192\varepsilon^2$	$3.192\varepsilon^2$	$0.500\varepsilon^{-1}$	$0.500\varepsilon^{-1}$	$1.949\varepsilon^2$	$1.771\varepsilon^2$	$0.820\varepsilon^{-\frac{2}{3}}$	$0.524\varepsilon^{-\frac{4}{3}}$
Lee, et al. 8)	0.3610 (0.336)	0.3250 (0.320)	1.486 (0.336)	1.486 (0.336)	0.1806 (0.304)	0.1625 (0.303)	1.812 (0.305)	2.578 (0.303)
Kotsvinos, et al. 7)	0.0808 (0.159)	0.1083 (0.184)	2.514 (0.199)	2.706 (0.185)	0.0808 (0.204)	0.1083 (0.247)	1.650 (0.351)	2.381 (0.322)
Rouse, et al.11)	——	——	——	——	0.1768 (0.301)	0.1562 (0.297)	1.800 (0.308)	2.600 (0.301)

Table 2 Comparison of liquid buoyant jet (axisymmeric case)

	Jet				Plume			
	$\frac{b}{x}$	$\frac{a}{x}$	$\frac{u_0 x}{\sqrt{m}}$	$\frac{\sigma_0 x}{q\sqrt{m}}$	$\frac{b}{x}$	$\frac{a}{x}$	$\frac{u_0 x^{1/3}}{(qg)^{1/3}}$	$\frac{\sigma_0 g x^{5/3}}{(qg)^{2/3}}$
Authors	$3.853\varepsilon^2$	$3.853\varepsilon^2$	$0.207\varepsilon^{-2}$	$0.207\varepsilon^{-2}$	$3.030\varepsilon^2$	$2.669\varepsilon^2$	$0.452\varepsilon^{-\frac{4}{3}}$	$0.175\varepsilon^{-\frac{8}{3}}$
10) Morton	0.1640 (0.206)	0.1902 (0.223)	4.865 (0.206)	4.240 (0.221)	0.0984 (0.180)	0.1141 (0.207)	4.872 (0.168)	11.74 (0.207)
1) Abraham	0.1125 (0.171)	0.1220 (0.178)	6.997 (0.172)	6.263 (0.182)	——	——	——	——
Rouse,11) et al.	——	——	——	——	0.1021 (0.184)	0.1187 (0.211)	4.700 (0.173)	11.00 (0.212)

In relation to the turbulent diffusivity, an entrainment coefficient is often used. Let us consider the entrainment coefficient in our case. In a two-dimensional case from the conservation equation of mass, an entrainment coefficient α can be given as

$$\frac{d}{dx}\{\frac{\sqrt{\pi}}{2} u_0 b\} = \alpha u_0 \tag{22}$$

by using the equations which correspond to the Eq.7 and Eq.9 but have the dimensional form and eliminating $d/dx\ (u_0 b)$ from Eq.22, we have

$$\left.\begin{aligned} \alpha &= \sqrt{2}\varepsilon^2 + 2a^2\sigma_0 g/(\sqrt{\pi} b u_0^2) - \sqrt{2}a\sigma_0 g/(\sqrt{\pi} u_0^2) \\ &= \sqrt{2}\varepsilon^2 + \sqrt{1+\lambda^2}(2\lambda - \sqrt{2})\pi^{-1} R_i\ ,\ R_i = qg/u_0^3 \end{aligned}\right\} \tag{23}$$

α changes with Ri, and the asymptotic a value of α for a jet and plume can be given from the corresponding Ri value, Ri=0 and 0.8207^{-3} respectively.

In the case of an axisymmetric buoyant jet, the entrainment coefficient is defined as

$$\frac{d}{dx}(\pi u_0 b^2) = \alpha \cdot 2\pi b u_0 \tag{24}$$

Making use of the same procedure as used in deriving Eq.23, from Eqs.15, 17, 19 and 20, we have

$$\alpha = (2 + \sqrt{2})\varepsilon^2/\sqrt{\pi} + \lambda\{\lambda + (\lambda - 1)(1 + \sqrt{2})\}/(2F_{dc}^2) \quad (25)$$

$$F_{dc} = u_0/\sqrt{a\sigma_0 g}$$

Like a two-dimensional case, α varies with buoyant jet behavior, represented by F_{dc} in this case. List and Imberger (9) give the following expression in a two-dimensional case,

$$\alpha = 0.055 + 0.087R_i/\sqrt{2} \quad (26)$$

and Wright (14) gives also for an axisymmetric case

$$\alpha = 0.057 + 0.25/F_{dc}^2 \quad (27)$$

Some other expressions, like Eq.26 or Eq.27, by other researchers (3),(4),(7),(9),(12),(14) were given.
Eq.23 and Eq.25 are derived by use of mixing length theory and by the assumption that ε in Eq.6 is constant all over a buoyant jet. It is not the objective in this study to investigate the effect of density gradient on a turbulent structure, so further consideration is not done on this matter.

EXPERIMENTAL INVESTIGATION

Experimental set up.

To examine the validity of theoretical investigation, particle laden vertical buoyant jet experiments are performed in a rectangular large water tank T which has 5.0m length, 2.0m width and 2.0m full depth. A schematic diagram of the experimental equipment is shown in Fig 12.

In two-dimensional experiments, it is necessary to avoid the secondary flow caused by the jet. For this purpose a vertical plate D is set 10cm apart from a wall, with opening at both side, which allows suitable in or out side flow at each edge of the experimental field between a basin wall and this plate. The jet nozzle N1 of 9.8cm width and 0.3cm apparture is set at the middle of the channel-water surface.

For an axisymmetric jet, circular nozzle N2 of 1.3cm in diameter is placed at the center of a tank water surface.

The tap water discharged from a tank W is mixed with sand particles in a tank M Water volume flux is controlled by valves V1, V2 and V3, the particle feed rate is controlled by changing the revolution of the feeding roller installed in the hopper H. A total jet flux is controlled by valve V4 or V5 and V6.

Sand particles used have specific gravity of 2.65, and are passing through a 70 mesh (0.210mm in opening) sieve and are retained on the 100 mesh (0.149mm) sieve. They have mean fall velocity of 2.5cm/sec.

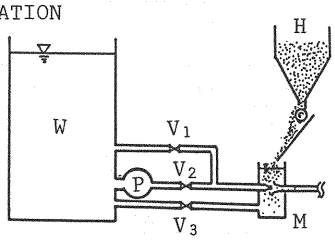

Fig.12-1 Schematic diagram of experimental arrangement (water and particles supply)

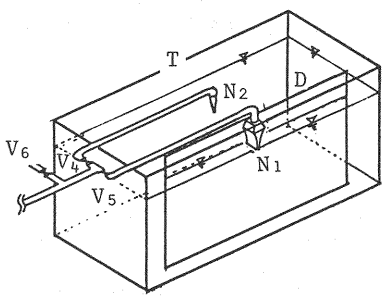

Fig.12-2 Schematic drawing of experimental arrangement (large tank and jet nozzle)

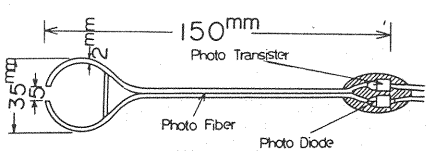

Fig.13 Photoelectric probe of a turbidty meter

Table 3 Experimental conditions (two-dimensional case)

RUN	$m(\frac{cm^3}{s^2})$	$q(\frac{cm^2}{s})$	M	Q	SYMBOL
2-1	1920	0.4083	65.42	529.2	
2-2	981	0.2423	46.20	314.0	
2-3	824	0.2746	50.22	355.9	
2-4	480	0.1157	28.23	150.0	
2-5	380	0.1232	29.43	159.6	
2-6	307	0.1885	39.08	244.3	
2-7	309	0.5399	78.81	699.7	
2-8	307	0.4628	71.11	599.7	
2-9	309	0.5206	76.92	674.7	

Table 4 Experimental conditions (axisymmetric case)

RUN	$m(\frac{cm^4}{s^2})$	$q(\frac{cm^3}{s})$	M	Q	SYMBOL
3-1	3963	1.4530	139.9	1656.4	
3-2	2357	1.0960	136.9	1603.2	
3-3	8173	1.3440	90.1	856.0	
3-4	7669	1.6410	113.6	1212.1	
3-5	2324	1.6150	203.1	2895.4	
3-6	9987	1.3850	84.0	770.6	
3-7	3373	1.4140	147.6	1794.0	
3-8	3216	2.3520	251.5	3988.9	
3-9	8618	2.2990	150.2	1841.2	
3-10	8650	0.5579	36.3	219.4	

The velocity in a jet is measured by use of a pitot tube of 3.0 mm diameter and a pressure gauge unit.

Sediment concentrations are measured by a hand made turbidity meter with photo-electric probe, shown in Fig.13 . Experiments were carried out by changing the several jet conditions. Experimental conditions in each run are summarized in Table 3. and 4.

Experimental results

Examples of flow velocity profiles and of sediment concentration profiles across a jet axisis are shown in Fig.2 for a two-dimensional case and in Fig.3 for an axisymmetry one together with theoretical curves. Because of the difficulty of precise measurement and the sensitivity of disturbances, the data was scattered. The theoretical curve, however, fits to the experimental data, so that the jet profiles have the similarity.

The center-line value of u and σ are shown in Fig.4 and 5 in two-dimensional case, and in Fig.8 and 9 in axisymmetric one. In these figures experimental data by other researchers are also shown. For the data by Kikkawa et al. (5), Q is 120 and ε=0.19 and for the data by Kitano et al, ε is taken to be 0.3 . For the Brush (2), Singamsett (13) data which investigate the momentum predominant jet behavior, ε=0.17 is used.

To compare the theoretical value with experimental results, we used following numerical values of ε; ε=0.23 for two-dimensional case and ε=0.18 for axisymmetric case. In order to obtain better agreement with our experimental results, for two-dimensional case, two values of may be used, ie. ε=0.20 in jet-like region, ε=0.25 in plume-like region. But it must be noted that the values of all characteristic parameters varies with ε , and it becomes difficult to give any practical meaning to the absolute values of X, when ε varies with X.

The jet spreading width is also shown in Fig.6 for a two-dimensional and in Fig.10 for an axisymmtric case to check the theoretical value.

Several papers (1), (5), (7), (10), (11), (13) report that the λ=A/B>1, this means the sediment spread wider than momentum, on the other hand some experimental results show that λ is less then unity (6), (2), (11), (8) . We assumed in this study that the rate of the mixing length of momentum is equal to that of sediment, but this assumption may need more careful works to understand precisly.

Considering the hardness of experiment especially of the sediment concentration measurement, it can be said from these figures that the theoretical curves fit to the experimental results.

SUMMARY AND CONCLUSION

We discussed particle laden jet which is injected vertically into still water of uniform density. The basic equations are derived from the conservation of volume, momentum and gravitational flux of sediment. Similarity profiles of jet flow velocity and of sediment concentration are assumed and Prandtl's mixing length hypothesis is applied to the turbulent diffusivity.

The general procedure employed in the theoretical analysis consist of integrating conservation equations for momentum and negative buoyancy over the jet cross section. Moment transformations of these conservation equations are also used to get numerical solutions.

Numerical solutions show that the buoyant jet performs like pure jet near the jet source, as the initial momentum is predominant. This jet turns to the plume as the jet velocity decrease and relative density becomes predominant along the jet axis.

For the two-dimensional case, the velocity of this plume becomes asymptotic to a finite value, on the other hand in a round jet this velocity decreases continuously along the jet. Therefore in a round jet this plume turns to the next stage, where settling of particles becomes predominant. As we discussed the jet from point source or line source, the variations of the buoyant jet properties along jet axis are determined uniquly only by Q, which is non-dimensional sediment flux.

The validity of numerical solutions are checked by laboratry experiments.

ACKNOWLEDGEMENT

The authors wish to express their thanks to a graduated student S.Shirahama by his help in performing experiments.

The work was partly supported by a Research Grant of Ministry of Education, Science and Culture, and also by a Research Fund of the graduates' association of Kyushu Institute of Technology, Meisenkai.

REFERENCES

1. Abraham, G : Jet Diffusion in liquid of greater density, J.Hydraul. Div. ASCE, Vol.86 No. HY6, pp.1-13, 1960
2. Brush, L.M.Jr : Exploratory study of sediment diffusion, J.Geoph. Research, Vol.67, No.4, pp.1427-1433, 1962
3. Fox,G.D : Forced plume in a stratified fluid, J.Geoph.Research, Vol.75, No.33, pp.6818-6834, 1970
4. Hirst,E: Buoyant jets discharged to quiescent stratitied ambients , J. Geoph. Research. Vol.76, No.30, pp.7375-7885, 1971
5. Kikkawa, H. , Fukuoka, S. , and Yoshikawa, K. : A study of fluid-solid particles interaction, Proc. Japan Soc. Civil Eng., Vol.260, pp.89-100, 1979 (in Japanese).
6. Kitano, Y., Tanaka, M., and Awaya, Y : Some properties of bubble jet in still water, Proc. Japan Soc. Civil Eng., Vol.253, pp.37-47, 1976. (in Japanese)
7. Kotsovinos, N. E., and List, E. J. : Plane turbulent buoyant jets, Part.1 Integral properties, J. Fluid Mech., Vol.81, Part.1, pp.22-24, 1977
8. Lee. S. L., and Emmons, H. W. : A study of natural convection above a line fire : J. Fluid Mech., Vol.11, pp.353-368, 1961
9. List, E. J., and Imberger, J : Turbulent Entrainment in Buoyant Jets and Plumes, J. Hydraul. Div. ASCE, Vol.99, pp.1461-1474, 1973
10. Morton, B. R. : Forced plumes, J. Fluid Mech., Vol.5, pp.151-163, 1959
11. Rouse, H., Yih, C. S., and Humplreys, H. W. : Gravitational Convection from a Boundary Source, Tellus, Vol.4, pp.201-210, 1952
12. Scorer,R.S: Environmental Aerodynamics, Ellis Horwood, pp.320-321, 1978

13. Singamsetti, S. R. : Diffusion of sediment in a submerged jet, J. Hydraul. Div. ASCE, Vol.92, No.HY2, pp.153-168, 1966
14. Wright, S. J., and Wallance, B : Two-dimensional buoyant jet in stratified fluid, J. Hydraul. Div. ASCE, Vol.105, No.HY11, pp.1393-1406, 1979

APPENDIX(I) - DERIVATION OF EQ.9

$$\frac{\partial u}{\partial x} + \frac{\partial v}{\partial y} = 0 \tag{1}$$

$$u\frac{\partial u}{\partial x} + v\frac{\partial u}{\partial y} = \sigma g + \frac{\partial}{\partial y}\left(l^2\left|\frac{\partial u}{\partial y}\right|\frac{\partial u}{\partial y}\right) \tag{2'}$$

$$u = u_0 \exp(-y^2/b^2) \tag{3}$$

$$\sigma = \sigma_0 \exp(-y^2/a^2) \tag{4}$$

from Eq.2'

$$\int_0^\infty u\frac{\partial u}{\partial x}\,ydy + \int_0^\infty v\frac{\partial u}{\partial y}\,ydy = \int_0^\infty \sigma g y dy + \int_0^\infty \frac{\partial}{\partial y}\left(l^2\left|\frac{\partial u}{\partial y}\right|\frac{\partial u}{\partial y}\right)ydy \tag{A1}$$

Each term of Eq.A1 can be integrated with use of Eqs.4 and 5

$$\begin{aligned}\int_0^\infty u\frac{\partial u}{\partial x}\,ydy &= \int_0^\infty u_0\exp(-y^2/b^2) \times \{\frac{du_0}{dx}\exp(-y^2/b^2) \\ &\quad + \frac{2y^3}{b^3}\frac{db}{dx}u_0\exp(-y^2/b^2)\}ydy \\ &= \frac{1}{4}u_0 b^2\frac{du_0}{dx} + \frac{1}{4}u_0^2 b\frac{db}{dx}\end{aligned} \tag{A2}$$

$$\begin{aligned}\int_0^\infty v\frac{\partial u}{\partial y}\,ydy &= [vuy]_0^\infty - \int_0^\infty vudy - \int_0^\infty yu\frac{\partial v}{\partial y}\,dy \\ &= -\int_0^\infty\int_0^y\left(-\frac{\partial u}{\partial x}\right)dy\cdot udy - \int_0^\infty yu\left(-\frac{\partial u}{\partial x}\right)dy \\ &= \int_0^\infty u_0\exp(-y^2/b^2)\int_0^y\left(\frac{du_0}{dx} + u_0\frac{2y^2}{b^3}\frac{db}{dx}\right)\exp(-y^2/b^2)dydy \\ &\quad + \int_0^\infty u\frac{\partial u}{\partial x}\,ydy \\ &= \left(\frac{\pi}{8} + \frac{1}{4}\right)u_0 b^2\frac{du}{dx} + \frac{\pi}{8}u_0^2 b\frac{db}{dx}\end{aligned} \tag{A3}$$

$$\begin{aligned}\int_0^\infty \frac{\partial}{\partial y}\left(l^2\left|\frac{\partial u}{\partial y}\right|\frac{\partial u}{\partial y}\right)ydy &= \left[l^2\left|\frac{\partial u}{\partial y}\right|\frac{\partial u}{\partial y}\cdot y\right]_0^\infty - \int_0^\infty l^2\left|\frac{\partial u}{\partial y}\right|\frac{\partial u}{\partial y}\,dy \\ &= -\int_0^\infty \varepsilon^2 b^2 u_0^2\left(\frac{2y}{b^2}\right)\left(\frac{-2y}{b^2}\right)\exp(-2y^2/b^2) \\ &= \frac{\sqrt{\pi}}{2\sqrt{2}}\varepsilon^2 u_0^2 b^2\end{aligned} \tag{A4}$$

$$\int_0^\infty \sigma g y dy = \sigma_0 g\int_0^\infty y\exp(-y^2/a^2)dy = \frac{a^2}{2}\sigma_0 g \tag{A5}$$

Substitution Eqs. A2, A3, A4, A5 into A1

$$(\pi + 4)u_0 b^2 \frac{du_0}{dx} + (\pi + 2)u_0^2 b \frac{db}{dx} = 2\sqrt{2\pi}\cdot\varepsilon^2 b u_0^2 + 4a^2\sigma_0 g \qquad (9')$$

The nondimensional expression of Eq.9' reduces to Eq.9. Eqs.10, 17 and 18 can be derived by using the same procedure.

APPENDIX (II) - NOTATION

The following symbols are used in this paper:

a, A	= characteristic jet width of suspended sediment;
b, B	= characteristic jet width of momentum;
c	= volume concentration of sediment particles;
F	= densimetric Froude Number;
g	= acceleration of gravity;
K	= eddy diffusivity;
Km, Ks	= eddy diffusivity for momentum and sediments ;
l	= mixing length;
L_0, L_1	= characteristic length of jet;
m, M	= kinematic source momentum flux of jet;
q, Q	= source volume flux of jet;
Ri	= Richardson Number;
u	= flow velocity in the x direction;
u_0	= the value of u along the centerline;
v	= velocity in the y direction;
w	= fall velocity of sediment particles;
x, X	= longitudinal coordinate taken along the jet axis;
y	= lateral coodinate;
α	= entrainment coefficient;
β	= reciprocal of turbulent Schmidt number;
ε	= 1/x , numerical constant;
λ	= a/b , jet width ratio;
ρ_s , ρ_1	= density of sediment particles or fluids; and
σ, S	= excess specific gravity due to particles suspension;